Lawrence Berkeley National Laboratory
LBL Publications

Title

Roof ponds combined with a water-to-air heat exchanger as a passive cooling system: Experimental comparison of two system variants

Permalink

https://escholarship.org/uc/item/84t1g397

Authors

Almodovar, José Manuel
La Roche, Pablo

Publication Date

2019-10-01

DOI

10.1016/j.renene.2019.03.148

Peer reviewed

eScholarship.org Powered by the California Digital Library
University of California

Roof ponds combined with a water-to-air heat exchanger as a passive cooling system: Experimental comparison of two system variants

Jose Manuel Almodovar[a], Pablo La Roche[b]

[a] School of Architecture, University of Seville, Spain
[b] Department of Architecture, Cal Poly Pomona University, United States

Abstract

This paper evaluates two roof pond configurations combined with a water-to-air heat exchanger (WAHE). Test cells of 1.35 m x 1.35 m x 1.35 m with the same thermal properties, except for the roofs, are built in a hot-dry climate with mild winters. They are connected with a WAHE placed inside the roof pond's water by a pipe through which the indoor air is re-circulated. The first roof consists of a 0.35 m deep water pond covered with a floating polystyrene insulation 0.03 m thick, and a spray system located 0.5 m above it that operates at night. The second roof is covered with an aluminum plate separated by a 0.10 m air gap above a 0.25 m deep water pond. We ran multiple series and compared the results to a control cell that had an energy code compliant insulated roof. Furthermore, predictive equations are developed to dimension the WAHE system. Results demonstrate that the cells with roof ponds have higher cooling performance than the code compliant control cell. The best performance is obtained in the cell with the WAHE operating all time. In this case, the indoor temperature stayed below 24 °C even with ambient temperatures above 35 °C.

Keywords: roof pond; water-to-air heat exchanger; passive cooling; evaporative cooling; thermal energy storage; physical testing – mockups.

1. Introduction

Buildings are responsible for around 35-40% of final energy consumption and about 35% of total GHG emissions [1]. The roof is the most exposed building envelope element to the sky. It has a great cooling potential due to heat dissipation through different processes such as evaporation, radiation, and conduction [2]. On the other hand, the roof can also account for excessive heat gains in hot periods due to the effect of the direct solar radiation. There is evidence that the roof alone is responsible for up to 50% of the heat loads in single-story buildings in hot climates [3].

Traditional systems to reduce solar gains through the roof are based on increasing the thickness, thermal mass and insulation, as well as adding shading elements and reflective finishes. However, the use of roof ponds for cooling purpose has some advantages over traditional systems due to the high thermal capacity of the water, which can reduce temperature swings and peak temperature [4].

The use of roof ponds was probably investigated for the first time in the 1920s at the University of Texas [5]. In 1978 Hay and Yellot [6] introduced the concept of a roof pond with the “skytherm” system, in which the cooling effect was obtained by nocturnal radiation. In 1994 Givoni [7] evaluated the performance of fixed shade and floating insulation roof pond systems under different climatic conditions. Furthermore, a novel thermo-active building systems harnessed from rainwater cisterns has been used for heating and cooling [8].

The number of publications on roof ponds has increased in the last years. Kharrufa & Adil [9] experimentally tested the cooling performance of a roof pond ventilated mechanically in a hot and dry climate with good results in terms of indoor air temperature and heat flux through the roof. Krüger et al. [10] simulated 37 cool roof variants alternating roof shape, materials and construction by using an algorithmic hybrid matrix. Tang & Etzion [11] developed a simulation model to evaluate a roof pod with gunny bags which is widely accepted as one of the most efficient roof cooling techniques. In addition, several authors have summarized the state of the art of roof pond variants [12-13].

Furthermore, the use of earth-to-air heat exchangers (EAHE) that use the ground for heat storage and dissipation has also increased. Due to the high thermal mass of the soil, temperature swings under the ground are smaller than at the surface level. After a certain depth, the soil temperature will be higher than ambient temperature in the winter and lower than the peak ambient in the summer. In a EAHE system, the air circulates through a buried pipe powered by a fan. In summer, the air circulating through the pipes is cooled because the soil temperature around the pipe is lower than the ambient temperature. Several models have been proposed to evaluate the thermal performance of a EAHE [14-15]. Benkert et al. [16] have developed the GAEA computer tool based on an experimentally validated physical-mathematical model. In addition, Ascione et al. [17] have evaluated the EAHE energy performance as a function of the main boundary conditions.

The water-to-air heat exchanger (WAHE) system that uses the water as a heat sink was patented by Richard Bourne and David Springer [18]. EAHE systems are increasingly being used, and few research has been carried out to evaluate the benefits of WAHE [19]. However, WAHE have some advantages compared to EAHE [20]. The water dissipates the heat exchanged through the pipe more easily than soil and water has a higher thermal capacity than earth.

The literature review suggests that considerable resources have gone in the last years into the study of roof ponds, but the combined effect of roof ponds with WAHE systems has not yet been studied. This paper experimentally evaluates the cooling performance of two roof pond configurations coupled directly (conductively) with the indoor space: a roof pond with a floating insulating panel and spray system operating at night, and a roof with a sealed flat aluminum plate separated from the water by an air gap. To do that, test cells were built with similar thermal envelope except for the roofs, and then experimentally tested in a hot-dry climate with mild winters. The effect of a WAHE system on the cooling performance of both roof pond variations were also tested. Results have been compared to a control cell that had an energy code compliant insulated roof. Furthermore, predictive equations are developed to apply the WAHE system to different buildings and climatic conditions.

2. Experimental systems

To evaluate the benefits of adopting different roof pond configurations combined with a WAHE system, test cells were built and monitored at the Lyle Center for Regenerative Studies in Cal Poly Pomona. The center is in a hot-dry climate with mild winters about 30 km east of Los Angeles, in southern California.

The test cells are 1.35 m x 1.35 m x 1.35 m, facing south, slightly to the west. The walls of the test cells are 178 mm thick, with drywall on the inside, 5.08 cm x 10.16 cm (2” x 4”) studs with glass wool insulation, OSB board, XPS insulation board, and plywood on the outside. The floor of the cell is made of OSB board and XPS insulation board. The U-value of the wall and floor is 0.308 W/m^2K and 0.299 W/m^2K respectively. The walls were painted white to reduce the heat gains. A double-glazed window (610 mm x 610 mm) was installed in the south wall, and was tested with and without shade. A 10.16 cm (4”) exhaust fan and intake flap was

installed separately for the ventilation, and 89 mm plastic wheels were installed under the cell to adjust direction and location of the cells.

The test cell layers with the thermal properties of the two roof pond configurations and the control cell are indicated in the table below (Table 1).

Table 1. Test cell layers and their thermal properties.

		Material	Thickness (mm)	Thermal conductivity (W/mK)	Overall U-value (W/m^2K)
Insulated roof pond		Polystyrene	30	0.033	
		Water	300	0.591	
		Water proofing liner	1	0.210	0.272
		Metal pan	2	44.000	
Aluminum roof pond		Aluminum sheet	1	0.610	
		Air space	100	0.233	
		Water	250	0.591	1.311
		Water proofing liner	1	0.210	
		Metal pan	2	44.000	
Control cell roof		Metal sheet	1	44.000	
		Water proofing liner	1	0.21	
		OSB	11	0.130	
		Air Space	38	0.233	0.306
		XPS	140	0.043	
		Drywall	11	0.180	
Wall section		Drywall	10	0.180	
		Glass wool	89	0.044	
		OSB	11	0.130	
		Vapor barrier	1	-	0.308
		XPS	51	0.043	
		Air space	13	0.079	
		Plywood	5	0.130	

2.1. Experimental configuration of the roof pond with floating insulation and sprayed at night

This roof has a pond that is 0.35 m deep covered by a floating polystyrene insulation. A spray is placed over the roof pond to circulate the water over the insulation during the nighttime (from 7 pm to 7 am) and, in turn, cool the water by radiation and evaporation. The floating panel is 3 cm thick because research has shown that additional thickness does not provide significant improvements [21]. The exterior surface of the insulating panel is white to reflect solar radiation and the paint provides some improvement in the re-radiation during the night. The spray is 0.5 m above the center of the water pond, the minimum height to provide some significant evaporative cooling [22]. The supporting roof is a metal deck that provides good thermal coupling with the space below (Fig. 1).

Fig. 1. Test cell with a roof pond with floating insulation and spray system.

The insulation panel prevents overheating of the water during the daytime while the water is naturally cooled at night by evaporation and thermal radiation to the sky. The insulated roof pond was developed by Givoni and then tested with La Roche [23]. Previous research has shown that the cooling effect of this system is higher than the sprayed but uncovered pond and is practically identical to a shaded and ventilated pond [24]. Also, when the ambient wet bulb temperature is higher than the pond temperature, the sprays warm the water [25]. For this reason, the spray operation is limited to night hours (from 7 pm to 7 am) to improve efficiency and reduce the pond evaporation rate. The evaporative cooling system does not cool the building directly and instead cools the water that absorbs the heat from the building (indirect evaporative cooling). There is no evaporation from the roof pond and no water waste during the daytime.

2.2. Experimental configuration of the roof pond with an aluminum plate separated from the water by an air gap

This roof pond variant is an evapo-reflective roof composed of a water pond, 25 cm deep covered with a flat aluminum plate with low emissivity and separated from the water by an air gap of 10 cm. The system is sealed to prevent water vapor from escaping outside. Therefore, no water waste by evaporation is produced. The upper surface of the aluminum sheet is painted white to enhance its reflective properties. At night, the temperature of the aluminum sheet falls below the temperature of the water, and therefore, the water vapor inside the roof condenses and falls by gravity. This way, heat is transferred outside the system. A previous dynamic mathematical model for other configuration of roof pond covered by an aluminum plate was developed by Bencheikh and Bouchair [26] that combined the advantages of roof ponds with low emissivity materials, such as aluminum. However, there is a lack of experimental evaluation of this kind of roof pond configurations. The roof pond is supported by a metal deck that provides good thermal coupling between the cell and the indoor air (Fig. 2).

Fig. 2. Test cells views. Left: roof pond with a sealed aluminum plate. Right: details of the roof with aluminum plate.

2.3. Water-to-air heat exchanger (WAHE) system description

The cooled water of the roof ponds is used to cool the interior of the test cells through the WAHE. A fan in the pipe connecting the test cells to the roof ponds circulates the indoor air of the experimental cells through a WAHE placed inside the roof pond's water. The heat from the building is transferred by convection to the underwater pipe which then exchanges this heat by conduction to the water. Finally, the cooled air is introduced into the test cell to reduce overheating.

A PVC pipe 10.16 cm (4") diameter wrapped with batt insulation, waterproofing and aluminum foil connects the test cells and the roof ponds. However, an uninsulated aluminum pipe under the water increases the pipe's thermal conductivity and the WAHE efficiency. We have selected an underwater aluminum pipe of 10.16 cm (4") diameter and 3.5 m length; 1.5 m/s flow velocity; and fan operating all the time (day and night) to continuously reduce the indoor air temperature.

Data loggers were installed in multiple locations in the test cells to monitor the dry bulb temperature, mean radiant temperature, and relative humidity. The sensors were Onset models U12-012, UX 120-006M, and TMC6-HD respectively. Data was recorded every five minutes. Temperature sensors had a measuring range from 0 to +100 °C, and an accuracy of ±0,5 °C. The calibration before the measurements guaranteed the proper functionality of the setup. Figure 3 shows their location in the test cells.

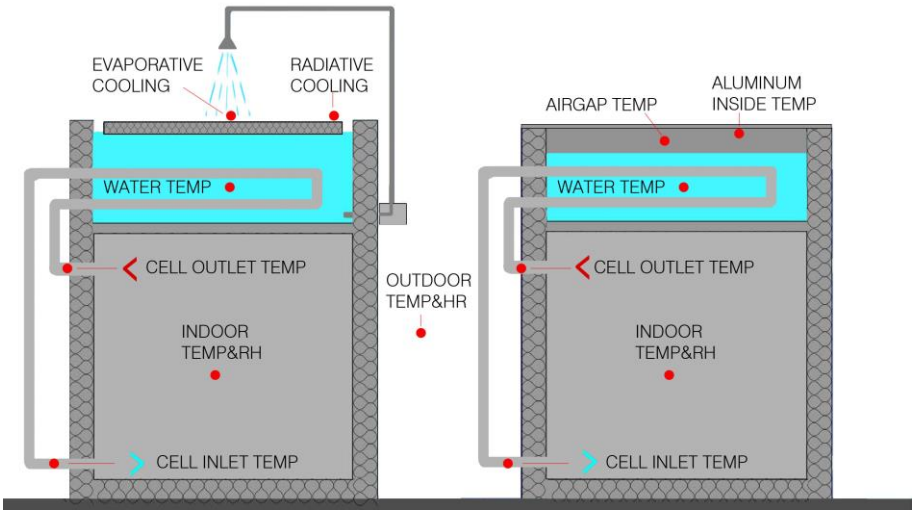

Fig. 3. Data loggers' location in the test cells. Red dots are temperature sensors.

3. Results

We have selected several series carried out from August to October 2016 to compare the results of both roof pond configurations to a control cell that had a California energy code compliant insulated roof. To evaluate the effect of the WAHE system in the performance of both roof pond variants we have carried out series with the WAHE both on and off. Due to the space limitation, only a few selected series are presented in this paper. The parameters used to evaluate the systems' efficiency are the roof pond's water cooling potential, the roof pond's effect in cooling the space coupled conductively below, the heat transfer efficiency through the WAHE, and the effect of the WAHE in improving the cooling performance of the roof ponds.

3.1. Results of the roof pond with a floating insulation and sprayed at night

3.1.1. The WAHE system des not operate (series 1)

This series, that started on August 31st, evaluates the cooling effect of the night-time spray system above the insulating panel to cool the water by evaporation and radiation to the sky and the cooling effect in the space coupled below by a metal plate. The WAHE system is not installed in this series.

Results show that the roof pond's water cooling is very effective (Fig. 4). During the nighttime, the water temperature is close to the minimum ambient temperature, usually below 20 ºC; while during the day the water temperature increases around 2 ºC above the nighttime value. In contrast, the ambient temperature can increase over 15 ºC during the daytime.

Maximum temperatures are a good indicator of the cooling performance of the system. The higher the difference between the inside and outside maximum air temperature, assuming a lower temperature inside the test cell, the better the performance. Results show that even with ambient temperatures above 35 °C the cell air temperature can be kept below 27 °C (8 °C less than outside), while the control cell maximum temperature is around 29 °C. Thus, the test cell has high performance, even better than the control cell that meets the California energy code.

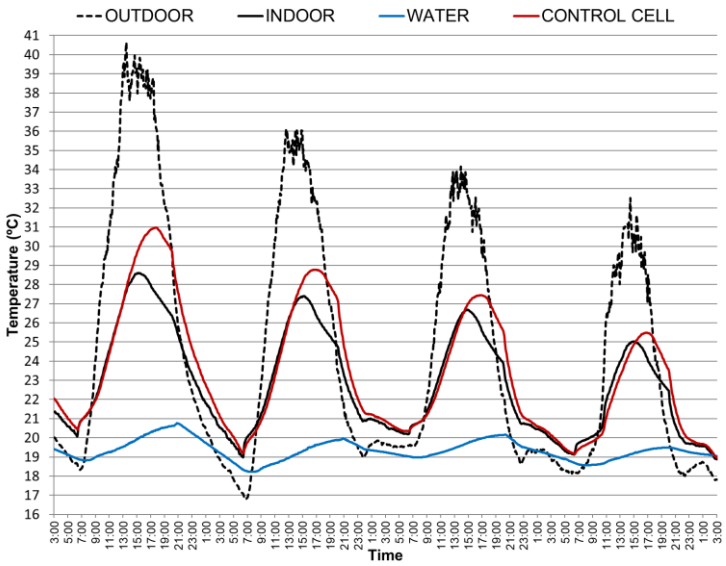

Fig. 4. Insulated roof pond with sprays working at night without WAHE, temperature measured over four days (series 1).

3.1.2. The WAHE system operates continuously (series 2)

This series, beginning on August 21st, investigates the same roof configuration than series 1 but with the WAHE system operating continuously (day and night). The results indicate that the system's performance improves considerably when the WAHE is operating. The maximum indoor temperature is below 24 °C while the ambient temperature is around 35 °C, a difference of more than 10 °C (Fig. 5).

The difference between the maximum pre-cooled air temperature at the pond outlet and the maximum water temperature is only around 1 °C. Therefore, the heat transfer, between the air circulating through the WAHE and the pond's water, is very effective. The rate of evaporation is 3.5 mm/day (so around 6.3 liters evaporated per day). On the other hand, results show that the air temperature in the cell outlet and pond inlet are almost identical, as well as the pond outlet and cell inlet. Therefore, the heat loss to the outside when the air circulates through the pipes connecting the interior of the cell and the pond water is negligible.

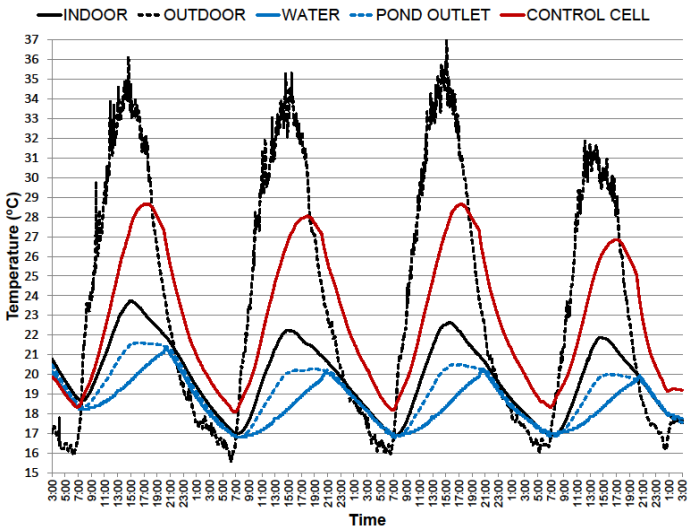

Fig. 5. Insulated roof pond with sprays working at night with WAHE operating all time, temperature measured over four days (series 2).

3.2. Results of the roof pond with an aluminum plate separated from the water by an air gap

3.2.1. The WAHE system do not operate (series 3)

In this series, beginning on July 26th, the maximum water temperature is slightly higher than the water temperature in the insulated roof pond with night sprays and the WAHE system turned off (series 1). However, the difference between the maximum outdoor and indoor temperature is still high, more than 6 °C when the ambient temperature reaches 35 °C. The experimental cell performance is also better than the control cell, with its maximum temperature more than 1 °C below the control (Fig. 6).

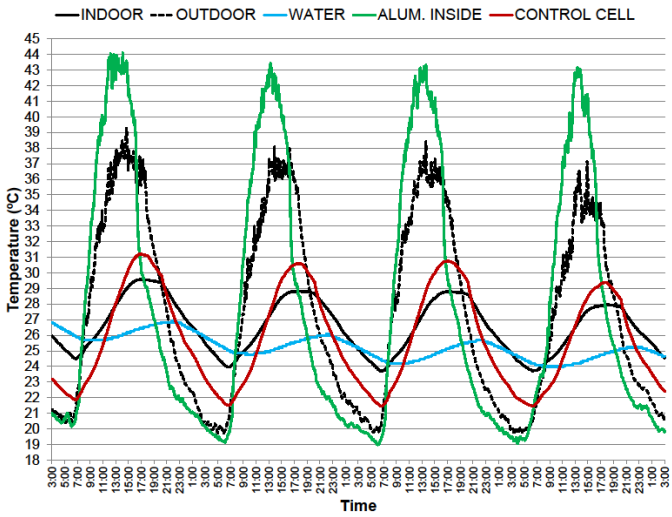

Fig. 6. Aluminum roof without WAHE, temperature measured over four days (series 3).

3.2.2. The WAHE system operates continuously (series 4)

This series that began on August 9th is similar to series 3 but with the WAHE system operating all day. The test cell maximum indoor temperature is now more than 2 °C below the control cell and the difference between the indoor and outdoor maximum temperature is more than 8 °C with an ambient temperature above 35 °C. Therefore, the WAHE improves the cooling performance of the roof pond. On the other hand, the heat exchange in the WAHE is as efficient as in series 2. The difference between the maximum pre-cooled air temperature and the water is only around 1 °C (Fig. 7).

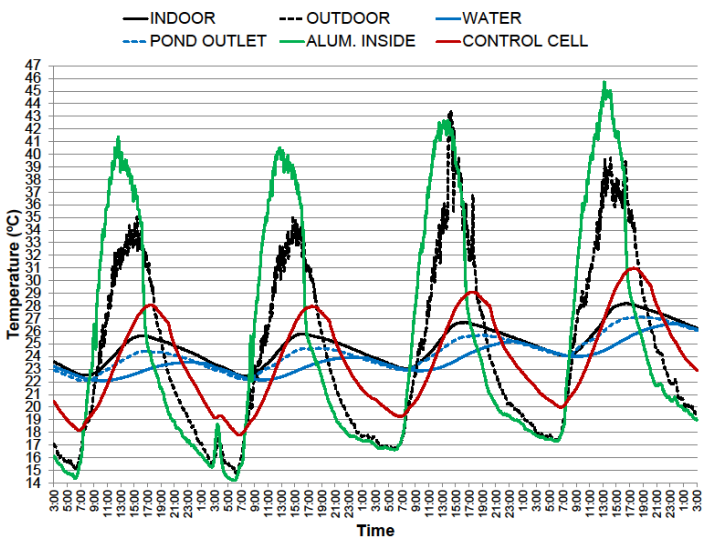

Fig. 7. Aluminum roof with WAHE operating all time, temperature measured over four days (series 4).

3.2.3. Sprayed at night and WAHE system operating continuously (series 5)

In this series, starting on August 14th, we tested the same system that in series 4 but with a spray system placed over the water and below the aluminum sheet, that operates at night, from 7 pm to 7 am (Fig. 8). Results show the cooling potential is lower than in series 4 (without sprays). When sprays operate at night the aluminum plate heats up, reaching a temperature of around 6 degrees more than when sprays do not operate. As a consequence, the aluminum inner surface temperature rises from a value close to the nighttime temperature to about only 1 °C below the roof pond's water temperature. Due to the overheating of the aluminum plate, the condensation process decreases, and consequently, also the cooling performance of the whole system (Fig. 8).

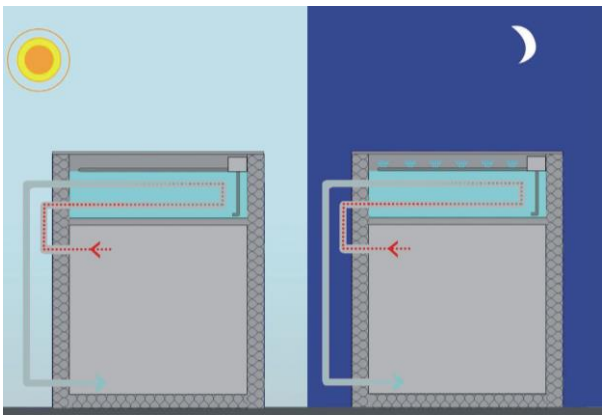

Fig. 8. Operation scheme of roof pond with aluminum plate, WAHE, and spray system running at night.

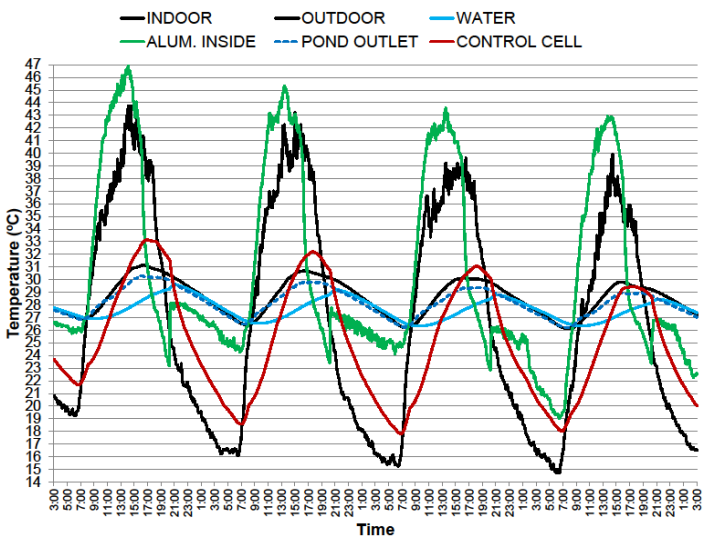

Fig. 9. Roof pond with aluminum plate, WAHE and spray system running at night, temperature measured over four days (series 5).

4. Comparison of experimental results

All series are compared with each other with a ratio that permits the comparison across different measurements, performed at different times. This number is called the temperature difference ratio (*TDR*) and was proposed by Givoni [24] with good results to compare passive

cooling systems with different configurations. *TDR* is determined by comparing the average reduction of the maximum temperature inside the cell with the average swing as expressed in the following equation:

$$TDR = (T_{max.amb} - T_{max.cell}) / (T_{max.amb} - T_{min.amb}) \quad (1)$$

Where: $T_{max.amb}$ = maximum ambient temperature (ºC); $T_{max.cell}$ = maximum cell temperature (ºC); $T_{min.amb}$ = minimum ambient temperature (ºC).

The numerator is the difference between the indoor maximum temperature and the outside maximum, and the denominator is the outdoor swing. A higher value indicates that there is a larger temperature difference between outside and inside and there is more cooling.
The TDR concept normalizes the capacity to reduce the indoor maximum temperature, as a function of the outdoor swing, permitting comparison of the different series at different times. For this equation to be descriptive of the different roof configurations there has to be a correlation between the indoor and outdoor maximum temperatures. Accordingly, we have compared experimental data obtained in the different roof pond configurations and the control cell using TDR as a function of the outdoor temperature swing (Figs. 10 to 12). Each point in figures 10 to 12 contains one day's data. Figure 10 compares data for the roof ponds with WAHE and the control cell, figure 11 shows data for different configurations of the insulated roof pond (INSU) and figure 12 shows data for different configurations of the roof pond covered with an aluminum plate (ALUM). A separate trend line is plotted for each series. In all of them TDR increases as the swing increases.

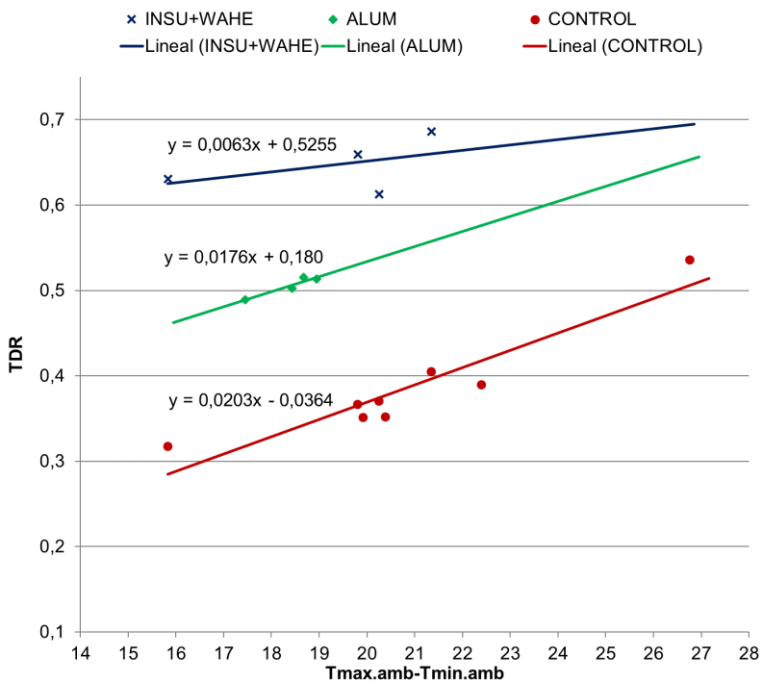

Fig. 10. Correlation between the daily outdoor temperature swing and the daily *TDR* in different roof pond configurations using WAHE and the control cell

Results show that the roof ponds perform better when the WAHE is operating. The best TDR in the experimental cells is in the insulated roof + WAHE which performs considerably better than the code compliant control cell, an average of around 0.23. The roof covered with aluminum + WAHE performs 0.6 worse than the insulated roof + WAHE, yet performs much better than the control cell, an average of about 0.17 (Fig. 10).

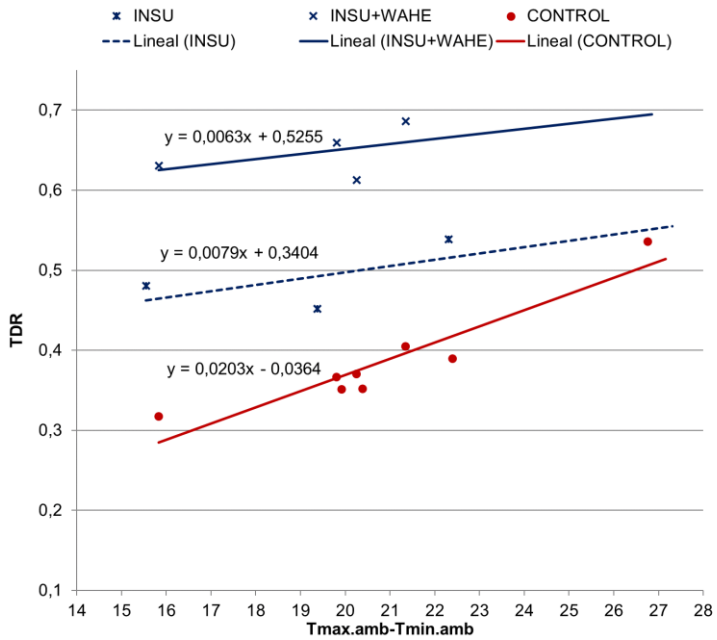

Fig. 11. Correlation between the daily outdoor temperature swing and the daily *TDR* in the insulated roof pond (INSU) with and without WAHE and the control cell

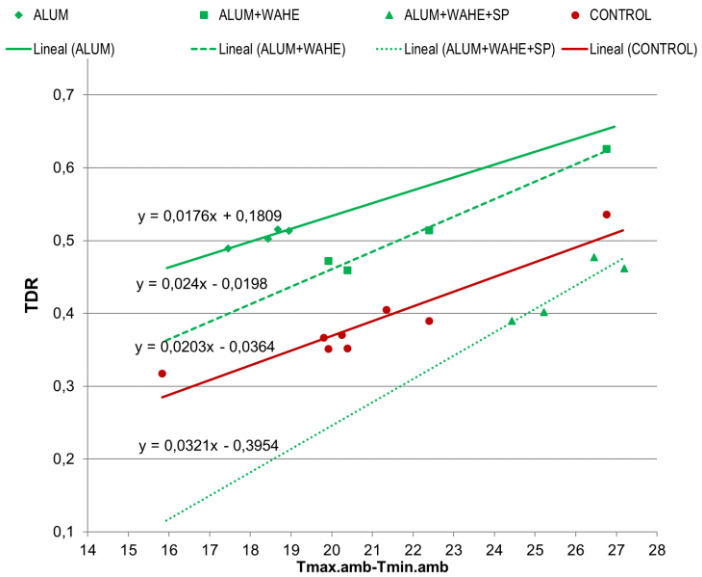

Fig. 12. Correlation between the daily outdoor temperature swing and the daily *TDR* in the different configurations of roof pond covered with aluminum (ALUM) with and without WAHE and the control cell

Due to the high cooling potential of the WAHE, the roof ponds' performance considerably decreases when it is not operating. Figure 11 shows that the insulated roof pond decreases around 0.12 when the WAHE does not operate, but nevertheless performs better than the control cell. The aluminum-covered roof pond decreases around 0.04, yet has better performance than the control cell. Only the roof covered with aluminum with sprays working at night has worse performance than the control cell (Fig. 12).

5. Predictive equation for system dimensioning

5.1. Temperature difference ratio (TDR) prediction

Based on the experimental results, the equations that predict the *TDR* in each system configuration are listed below.

Insulated roof pond with sprays (INSU):
$TDR = 0.0024(T_{max.amb} - T_{min.amb}) - 0.0198$ (2)

Insulated roof pond with sprays and WAHE (INSU+WAHE):
$TDR = 0.0063(T_{max.amb} - T_{min.amb}) - 0.5255$ (3)

Roof pond covered with aluminum plate (ALUM):
$TDR = 0.0176(T_{max.amb} - T_{min.amb}) - 0.1809$ (4)

Roof pond covered with aluminum plate and WAHE (ALUM+WAHE):
$TDR = 0.0203(T_{max.amb} - T_{min.amb}) - 0.0364$ (5)

After *TDR* is calculated for a building using Eqs. (2) to (5), it is possible to predict the indoor maximum temperature using Eq. (1) and solving for $T_{max,cell}$.

$T_{max.cell} = T_{max.amb} - [TDR * (T_{max.amb} - T_{min.amb})]$ (6)

Where outdoor maximum and minimum temperatures, or daily temperature swing, must be known. These simple equations derived from the experimental work permit us to calculate internal maximum temperatures as a function of outdoor maximum temperature and daily swing. They could be used in buildings with lightweight walls, south facing shaded windows and the selected roof pond prototype to predict maximum indoor temperatures.

More series should be performed under more extreme conditions to determine the applicability limits of the different roof pond configurations. Since the thermal mass of the pond water is used to improve the efficiency of the system, both the insulated roof pond and the roof pond covered with aluminum plate work well in the psicrometric zones for high mass and high ventilation. Thus, until more series are performed it is probably safe to assume that the applicability zone should be similar to that indicated in Givoni and Milne's chart (Fig. 13).

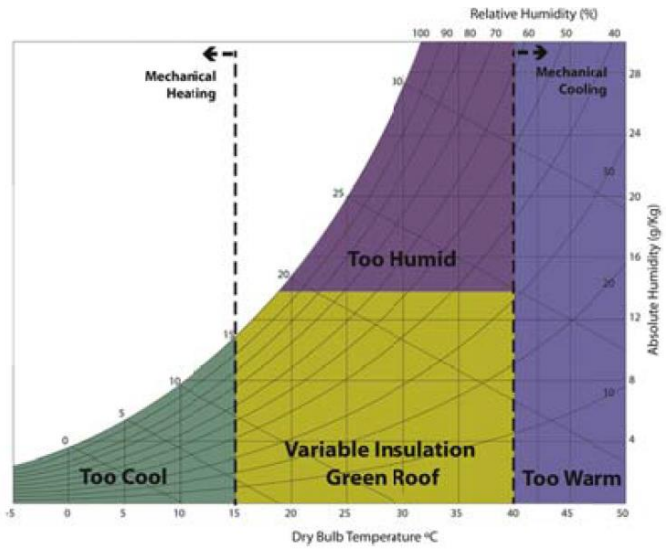

Fig. 13. Applicability of the roof ponds

5.2. Estimation of air temperature circulating through the WAHE

The indoor air, which is re-circulated from the test cell through the WAHE, transfers heat to the underwater pipe inner surface by convection, then the heat is transferred from the pipe inner to outer surface by conduction and finally by convection is transferred to the roof pond's water. The water acts as a heat sink that absorbs and dissipates the heat to the exterior which is the final heat sink. The overall thermal exchange though the WAHE between air and water in a segment of the underwater pipe is expressed by the equation:

$$dQ(L) = U\Delta T = \frac{T_a(L) - T_w}{R_t L} \quad (7)$$

Where $dQ(L)$ is the heat exchange of the pipe at the distance *L* from the pipe inlet (W), U is the heat transfer coefficient (W/°C), $T_a(L)$ is the air temperature of the pipe at the distance L from the pipe inlet (°C), T_w is the water temperature (°C), L is the pipe length (m), and R_t is the overall thermal resistance (°C/W).

The overall thermal resistance may be formulated by the sum of the thermal resistance values shown below:

$$R_t = R_1 + R_p + R_2 \quad (8)$$

$$R_1 = \frac{1}{2\pi r_i L h_1} \quad (9)$$

$$R_p = \frac{1}{2\pi L K_p} ln\left(\frac{r_o}{r_i}\right) \quad (10)$$

$$R_2 = \frac{1}{2\pi r_o L h_2} \quad (11)$$

Where R_1 is the thermal resistance due to convection heat transfer between the air in the pipe and the pipe inner surface (°C/W), R_p is the thermal resistance due to conduction heat transfer between the pipe inner and outer surface (°C/W), R_2 is the thermal resistance due to convection heat transfer between the water and the pipe outer surface (°C/W), r_i is the inner pipe radius (m), r_0 is the outer pipe radius (m), *L* is the pipe length (m), and K_p is the thermal conductivity of the pipe (W/m°C).

The convective heat transfer coefficient at the inner pipe surface $(\mathrm{W/m2°C})$, h_1, can be expressed by the following expression:

$$h_1 = \frac{N_u K_{air}}{2r_i} \quad (12)$$

Where N_u is the Nusselt number, and K_{air} is the thermal conductivity of the air (W/m°C).

The convective heat transfer coefficient at the outer pipe surface (W/m^2°C), h_2, can be estimated as follow:

$$h_2 = \frac{N_u K_w}{2r_o} \quad (13)$$

$$N_u = \left(0.60 + \frac{0.387 R_a^{\frac{1}{6}}}{\left(1+\left(\frac{0.559}{P_r}\right)\right)^{\frac{8}{27}}} \right)^2 \quad (14)$$

$$R_a = \frac{\delta \beta (\Delta T)(2r_o)^3}{\gamma \alpha} \quad (15)$$

Where K_w is the thermal conductivity of the water (W/m°C), R_a is the Rayleigh number, P_r is the Prandtl number, δ is the gravity (m/s), v is the kinematic viscosity of water (m^2/s), α is the thermal diffusivity of water (m^2/s), β is the thermal expansion coefficient of water (1/K), and ΔT is the temperature difference between the outer pipe and pond temperatures.

On the other hand, the thermal exchange between the air and the water through the WAHE system can be also expressed as a function of the mass air flow rate by the following equation:

$$dQ(L) = \dot{m} C_a dT_a(L) \quad (16)$$

Where C_a is the air specific heat (J/Kg°C).

The mass flow rate (Kg/s), ṁ, should be estimated as follows:

$$\dot{m} = \rho_a V A \quad (17)$$

Where $\dot{m}$ is the mass flow rate (Kg/s), ρ_a is the air density (Kg/m^3), V is the air velocity (m/s), and A is the pipe section (m^2).

Equating the thermal exchange through the WAHE as expressed in Eqs. (7) and (16), the following equations are obtained:

$$\frac{T_a(L) - T_w}{R_t L} = \dot{m} C_a dT_a(L) \quad (18)$$

$$\int_0^L \frac{-dL}{R_t L \dot{m} C_a} = \frac{dT_a(L)}{T_a(L) - T_w} \quad (19)$$

$$\frac{-1}{R_t \dot{m} C_a} = ln\left(T_{pond.out} - T_w\right)\Big]_{T_{pond.in}}^{T_{pond.out}} \quad (20)$$

Where $T_{pond.in}$ is the air temperature at the water pond inlet (°C), and $T_{pond.out}$ is the air temperature at the water pond outlet (°C).

By developing the previous equation, the air temperature at the pond outlet can be expressed as follows:

$$T_{pond.out} = T_w + \left(T_{pond.in} - T_w\right) e^{\frac{-1}{R_t \dot{m} C_a}} \quad (21)$$

It is assumed that the air temperatures at the cell outlet and pond inlet are equal because experimental measurements show that the heat loss through the pipe connecting the test cell and the water pond is negligible. As a consequence, $T_{pond.inl} = T_{cell}$. By replacing in Eq. (21), the $T_{pond.out}$ value may be expressed as follows:

$$T_{pond.out} = T_w + (T_{cell} - T_w) e^{\frac{-1}{R_t \dot{m} C_a}} \quad (22)$$

Where $T_{pond.out}$ is the air temperature at the water pond outlet (ºC), T_w is the water temperature (ºC), T_{cell} is the cell air temperature (ºC), R_t is the overall thermal resistance (ºC/W), $\dot{m}$ is the mass flow rate (Kg/s), and C_a is the air specific heat (J/KgºC).

Equation 22 estimates the air temperature at the WAHE outlet as a function of the test cell temperature, the air velocity, and the underwater pipe characteristics (length, diameter and material). Therefore, can be used to determine the impact of the different WAHE system elements in the reduction of the air temperature circulating through the WAHE.

5.3. System dimensioning according to the building thermal envelope and climatic conditions

A mathematical model for the dimensioning of the system as a function of the outdoor temperature swing for a specific location and the thermal envelope properties of the building have been developed in this research.

The thermal exchange of a test cell is determined by the following equation:

$$Q_{cell} = \sum_i U_i A_i \, (T_{amb} - T_{cell}) \tag{23}$$

Where U_i is the heat transfer coefficient of each envelope element (W/m^2°C), A_i is the Area of each envelope element (m^2), T_{amb} is the ambient temperature (°C), and T_{cell} is the air cell temperature (°C).

On the other hand, the thermal exchange through the WAHE can be expressed by the equation:

$$Q_{wahe} = \dot{m} C_a \left(T_{cell} - T_{pond.out}\right) \tag{24}$$

In a steady state, the heat exchange of the test cell, expressed in Eq. (23), is equal to the heat transferred to the WAHE, Eq. (24). Therefore, considering $Q_{cell} = Q_{wahe}$ the following equation may be formulated:

$$\sum_i U_i A_i \, (T_{amb} - T_{cell}) = \dot{m} C_a \left(T_{cell} - T_{pond.out}\right) \tag{25}$$

By replacing in Eq. (25) the Eq. (22), that express the air temperature at the roof pond outlet as a function of the underwater pipe characteristics (length, diameter and material) and the air flow rate, it is obtained that

$$\sum_i U_i A_i \, (T_{amb} - T_{cell}) = 2\dot{m} C_a \left(T_{cell} \left(1 - e^{\frac{-1}{R_t \dot{m} C_a}}\right) + T_w \left(e^{\frac{-1}{R_t \dot{m} C_a}} - 1\right)\right) \tag{26}$$

Where U_i is the heat transfer coefficient of each envelope element (W/m^{2}ºC), A_i is the area of each envelope element (m^2), T_{amb} is the ambient temperature (ºC), T_{cell} is the cell air temperature (ºC), $\dot{m}$ is the mass flow rate (Kg/s), C_a is the air specific heat (J/KgºC), R_t is the overall thermal resistance (ºC/W), and T_w is the water temperature (ºC).

By using Eq. (26), it is hence possible to dimension the WAHE system for different thermal envelopes and climatic conditions, i.e., the pipe length, diameter and material for different air flow rates. The water temperature must be estimated as a function of the roof pond configuration. The outdoor temperature swing for the specific location and thermal properties of the building envelop must be known.

We have plotted in figure 12 results obtained by applying the Eq. (26). Air flow rates from 1 to 5 m/s have been considered; and an aluminum underwater pipe, maximum indoor

temperature of 25 °C and water temperature of 22 °C have been selected. The y-axis shows the $\sum_i U_i A_i \ \Delta T$ value; where $\sum_i U_i A_i$ characterized the thermal envelope properties of the building and ΔT is the difference between the maximum ambient temperature and the maximum indoor comfort temperature. When the building envelope and climatic conditions have been selected, the required pipe length can be determined as a function of the pipe diameter which is indicated on the x-axis.

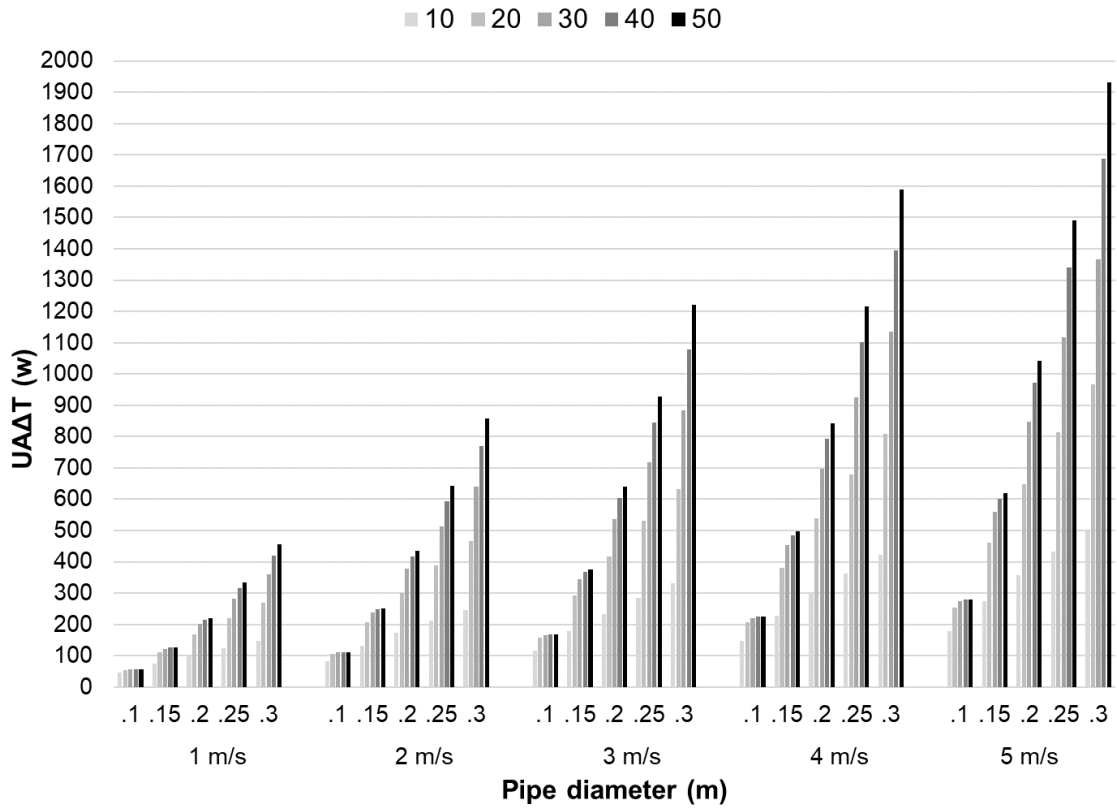

Fig. 11. Pipe length as a function of the $\sum_i U_i A_i \ \Delta T$ and pipe diameter for an air flow from 1 to 5 m/s. An aluminum pipe, maximum indoor temperature of 25 °C and water temperature of 22 °C have been considered.

The following considerations emerged from the graph:

For the range of air flow rate that we have considered, the higher the air velocity the lower the required underwater pipe length and/or diameter because more cool air is introduced into the test cells. As a result, the overall system efficiency increases. An air velocity higher than 5 m/s is not advisable in indoor spaces.

The amount of heat exchanged between the water and the air increases with the length of the underwater pipe. Therefore, the longer the pipe the greater the system performance. The impact of the pipe length in the system increases when the diameter is greatest. For instance, when the pipe length doubles from 10 to 20 m, system performance is only around double. For smaller pipe diameters the increase of the pipe length led to little or almost no performance improvement. Therefore, in most cases it is more advisable to use several short pipes instead of one longer pipe. Thus, it is not necessary to construct a large roof pond to house lengthy pipes.

As expected, the larger the pipe diameter the shorter the required pipe length because the amount of cool air entering the cell is increased. The data confirms that the pipe diameter is more important than its length. However, the depth of the roof pond limits the maximum pipe diameter. Thus, the economic cost and practical limitations must be balanced in each case.

For example, in the case of a space with the same thermal envelope than the test cells but a dimension of 3 m x 3 m x 3 m and a window size of 1 m x 1 m, $\sum_i U_i A_i$ is equal to 16.285 W/K. Considering a maximum indoor temperature of 25 ºC and maximum outdoor temperature of 35 ºC, $\sum_i U_i A_i \ \Delta T = 162.85$ W. We will assume an air flow rate of 5 m/s, water temperature of 22ºC and the same flexible aluminum pipe adapted in coil to the pond space that we used in the experimental evaluation. For a pipe diameter of 10.16 cm (4") almost two pipes of 5 m length is required. However, If the pipe diameter is twice, 20.32 (8"), only 1 pipe slightly less than 5 m length is necessary, and therefore is more cost effective.

6. Conclusion

Previous papers have demonstrated the cooling potential of different roof ponds coupled directly (conductively) with the indoor space for dissipating heat from the building, either by nocturnal long wave radiation to the sky, simple convection to exterior ambient air and evaporative cooling. However, there is a lack of studies about the combined effect of roof ponds and WAHE systems. This paper evaluated two roof ponds configurations and demonstrates that their performance is better than a code compliant insulated roof. In addition, their cooling potential is considerably improved using a WAHE system that re-circulates de indoor air between the cell and the roof pond.

Results show that the best performance is obtained by the floating insulation roof with sprays at night and WAHE system operating all time (0.23 TDR better than code compliant). This roof configuration can keep the indoor temperature under 24 °C even with outdoor temperatures above 35 °C, a difference of more than 10 °C. When the WAHE is not operating the system cooling potential decreases an average of 0.12. The efficiency of the roof pond covered with an aluminum plate is an average of 0.09 better than the control cell. This percentage is improved to around 0.12 TDR when the WAHE system operates.

Predictive equations to determine indoor temperature and to dimension the WAHE system for different thermal envelopes and climates were developed. There is good agreement between the measured experimental results and the simulation predictions.

Future research should include more series to experimentally evaluate other roof pond configurations with a fan sensor that re-circulates the indoor air through the WAHE or provide natural ventilation as required according to seasonal and daily variations. In addition, new development of predictive equations and mathematical models should be developed to apply the system to different buildings and climatic conditions.

Acknowledgements

This project was supported by a SPICE Grant from Cal Poly Pomona. The authors want to express gratitude to the John T. Lyle Center for Regenerative Studies at Cal Poly Pomona for its continuous support through their facilities. Moreover, they want to express their gratitude to Dongwoo Yeom and Brandon Gullotti for the construction of the test cells.

References

[1] P. La Roche, U. Berardi, Comfort and energy savings with active green roofs, Energy Build. 82 (2014) 492-504, https://doi.org/10.1016/j.enbuild.2014.07.055.

[2] S. Alvarez, J.L. Molina, Cooling by natural sinks, in: M. Santamouris (Ed.), Solar Thermal Technologies for Buildings: the State of the Art, Earthscan, Oxon, 2013, pp. 140-63.

[3] N.M. Nahar, P. Sharma, M.M. Purohit, Studies on solar passive cooling techniques for arid areas, Energy Convers. Manag. 40 (1999) 89–95, https://doi.org/10.1016/S0196-8904(98)00039-9.

[4] P. La Roche, Carbon-neutral architectural design, CRC Press, Boca Raton, FL, 2012.

[5] J. Cook, Passive cooling, MIT Press, London, 1985.

[6] H. R. Hay, J. Yellot, Natural air conditioning with roof pools and movable insulation, ASHRAE Trans. 75 (1978) 165–172.

[7] B. Givoni, Passive and low energy cooling, Van Nostrand Reinhold, London, 1994.

[8] D.E. Kalz, J. Wienold, M. Fischer, D. Cali, Novel heating and cooling concept employing rainwater cisterns and thermos-active building systems for a residential building. Applied Energy 87 (2010) 650-660.

[9] S.N. Kharrufa, Y. Adil, Roof pond cooling of buildings in hot arid climates, Build. Environ. 43 (2008) 82-89, https://doi.org/10.1016/j.buildenv.2006.11.034.

[10] E. Krüger, L. Fernandes, S. Lange, Thermal performance of different configurations of a roof pond-based system for subtropical conditions, Build. Environ. 107 (2016) 90-98, https://doi.org/10.1016/j.buildenv.2016.07.021.

[11] Runsheng Tang, Y. Etzion, On thermal performance of an improved roof pond for cooling buildings, Build. Environ. 39 (2004) 201-209, https://doi.org/10.1016/j.buildenv.2003.09.005.

[12] A. Sharifi, Y. Yamagata, Roof ponds as passive heating and cooling systems: A systematic review, Appl. Energy 160 (2015) 336–357, https://doi.org/10.1016/j.apenergy.2015.09.061.

[13] A. Spanaki, T. Tsoutsos, D. Kolokotsa, On the selection and design of the proper roof pond variant for passive cooling purposes, Renew. Sustain. Energy Rev. 15 (2011) 3523–3533, https://doi.org/10.1016/j.rser.2011.05.007.

[14] C. Peretti, A. Zarrella, M. De Carli, R. Zecchin, The design and environmental evaluation of earth-to-air heat exchangers (EAHE). A literature review, Renew. Sustain. Energy Rev. 28 (2013) 107-116, https://doi.org/10.1016/j.rser.2013.07.057.

[15] M.S. Sodha, Simulation of periodic heat transfer between ground and underground structures, in: A.A.M. Sayigh (Ed.), World Renewable Energy Congress VI, Pergamon, Brighton, 2000, pp. 965-968, https://doi.org/10.1016/B978-008043865-8/50194-X.

[16] S. Benkert, F.D. Heidt, D. Scholer, Calculation tool for earth heat exchangers GAEA, in: Proceedings of the Fifth International IBPSA (International Building Performance Simulation Association) Conference vol. 2, Prague, 1997.

[17] F. Ascione, L. Bellia, F. Minichiello, Earth-to-air heat exchangers for Italian climates. Renew. Energy 36 (2011) 2177-2188, https://doi.org/10.1016/j.renene.2011.01.013.

[18] R.C. Bourne, D.A. Springer, Energy-saving protected roof systems. Google Patents, 1992.

[19] H. Mroue, J.B. Ramos, L.C. Wrobel, H. Souhara, Experimental and numerical investigation of an air-to-water heat pipe-based heat exchanger, Appl. Therm. Eng. 78 (2015) 339-350, https://doi.org/10.1016/j.applthermaleng.2015.01.005.

[20] U. Berardi, P. La Roche, J.M. Almodovar, Water-to-air-heat exchanger and indirect evaporative cooling in buildings with green roofs, Energy Build. 151 (2017) 406-417, https://doi.org/10.1016/j.enbuild.2017.06.065.

[21] M. Tavana, R. Kammerud, H. Akbari, T. Borgers, A simulation model for the performance analysis of roof pond systems for heating and cooling, Lawrence Berkeley National Laboratory, 1980.

[22] S. Yannas, E. Erell, J.L. Molina, Roof cooling techniques: a design handbook, Earthscan, London, 2000.

[23] P. La Roche, B. Givoni, Indirect Evaporative Cooling with an Outdoor Pond, in: K. Steemers, S. Yannas (Eds.), Architecture, City, Environment: Proceedings of PLEA 2000, James & James, Cambridge UK, 2000, pp. 310-311.

[24] B. Givoni, Indoor temperature reduction by passive cooling systems, Sol. Energy 85 (2011) 1692-1726, https://doi.org/10.1016/j.solener.2009.10.003.

[25] E. Krüger, E. González, B. Givoni, Effectiveness of indirect evaporative cooling and thermal mass in a hot arid climate, Build. Environ. 46 (6) (2010) 1422-1433, https://doi.org/10.1016/j.buildenv.2009.12.005.

[26] H. Bencheikh, A. Bouchair, Passive cooling by evapo-reflective roof for hot dry climates, Renew. Energy 29 (2004) 1877-1881, https://doi.org/10.1016/j.renene.2003.12.021.